PHD IN BEHAVIORAL NEUROSCIENCE

PhD Program in Neuroscience - XXXI Cycle

Curriculum: Behavioral Neurophysiology

PREMOTOR CORTEX ENCODING OF DYNAMIC HAND FORCE AND MOTOR OUTPUT OBSERVATION UNDERLYING HAND-OBJECT INTERACTION

Supervisor: *Prof. Alexandra Battaglia-Mayer*   **PhD Student:** *Stefano Colangeli*

Academic Year 2017-2018

To my family

Summary

INTRODUCTION

Objects manipulation is a common daily action and a late achievement of evolution, which is unique to the primates lineage. It is subserved by a complex and distributed anatomo-functional system that specifies both hand configuration and force necessary to grasp and manipulate objects. Hand-object interaction has covered a prominent role in behavioral neurophysiology, raising fundamentals questions on how visuo-spatial and motor parameters are encoded and combined in the cerebral cortex.

From an historical perspective, the analysis of this function and of neural representation of movement in general was boosted by the introduction of the method, by Evarts (Evarts, 1968), of recording single cells activity from the cerebral cortex of behaving monkeys trained in specific motor tasks. The conceptual roots of this new and pioneering line of investigation were expressed in a coherent fashion ten years later by Thach (1978): "Theoretical requirements for the neural control of movement and posture, together with the motor deficits caused by ablation of the nervous system at different levels, have generated the theory that there are representations encoded in neural activity of abstract commands that govern volitional movement and posture, and that these commands descend from higher levels sequentially through adaptive stages to arrive at the muscles in a language appropriate for muscle control".

Under this perspective, it was natural to select force as a key parameter to be represented in motor cortex (MI), since MI has a direct access to the interneurons and motoneurons of the spinal cord though the pyramidal tract and force is developed by muscles activity. Not surprisingly, in Evarts's seminal study (1968), monkeys were trained to make flexion and extension movements at the wrist against loads that opposed or assisted movement, or to maintain postural fixation while resisting these loads. The conclusion was that neural activity of pyramidal tract neurons (PTNs), identified by antidromic stimulation at the bulbar pyramids, was related to the magnitude of force exerted by the animal, therefore to movement kinetics,

rather than to the position or displacement of the wrist, therefore to kinematics. A methodologically more advanced study, where direction, force and position were dissociated, concluded that these parameters were represented in equal fashion in M1 neural activity (Thach, 1978), without contending the crucial role of force. Relations between MI neural activity and muscle force were shown at about the same time by adopting precision grip tasks under isometric conditions, that allowed the study of force variation in absence of limb displacement, (Hepp-Reymond, 1978), and by Cheney and Fetz (1980), through spike-triggered averaging of EMG activity, that allowed to distinguish MI cells with monosynaptic connections with spinal motoneurons from those lucking such connections. The important conclusion of this study was that only M1 cells with monosynaptic connections to motoneurons encoded static force during a wrist flexion/extension task, therefore only layer V cortico-motoneuronal cells.

All above mentioned studies were based on tasks were force variation was confined at a single joint and spatial dimension, be it wrist flexion-extension, forearm supination-pronation, thumb-index finger opposition, therefore unable to fully capture the potential contribution to neural activity of the kinematic parameters, such as position direction, and velocity. Limb kinetics must be specified for all movements, and it representation in neural activity can only be appreciated in more naturalistic conditions, when movement unfolds over different spatial dimensions, such as hand reaching to visual targets.

Indeed, when for the first time hand movements were studied in a two-dimensional (2-D) space, it was found that cell activity in MI (Georgopoulos, et al., 1982) and posterior parietal area 5 (Kalaska et al., 1983) was related in an orderly fashion to the direction of reaches, since it was maximal in a preferred direction and decreased for directions further and further away from it. Most important, the broad directional tuning of MI cells suggested that reach direction could only be encoded through a population code, rather than by single cell activity (Georgopoulos, et al., 1983), given the broad, therefore ambiguous, directional tuning of individual neurons. In

addition, in both MI and area 5 cell activity was monotonically tuned to arm position in space (Georgopoulos et al., 1984; for a recent review, see Battaglia-Mayer, 2019).

Since force is a vector defined by its magnitude and direction, these results opened the way to further analysis of the relationships between cell activity, force and direction in the cerebral cortex. In this context, an important contribute came from studies by Kalaska's group (Kalaska and Hyde, 1985; Kalaska, et al., 1989), who have extended the analysis of the neural encoding of static force to the direction of 2-D multi-joint arm reaching. The conclusion of these studies was cell activity in MI was broadly tuned to the direction of static force.

However, the most compelling results came from an elegant and imaginative study (Georgopoulos et al., 1992) where monkeys were trained to exert 2-D directional forces under isometric conditions in presence of a constant bias force that mimicked the presence of gravity. This approach allowed to study the relationships between M1 cell activity and different forces, that were dissociated: 1) the amount of force exerted by the monkey, decomposed into a static and dynamic components, with the first equal and opposite to the bias force, the second corresponding to the net force; 2) the net force, which is necessary to move the hand in the desired direction against the bias force, therefore corresponding to the dynamic force; 3) the change of force over time. The result of this study was that population activity in M1 varied with the direction of the dynamical force and with the force change over time, but not with the amount of force exerted by the monkey. The authors of this study suggested that the force exerted by the subject and its magnitude could be encoded at the spinal level, thanks to the convergence of different supraspinal and propriospinal inputs.

The extension of these studies to posterior parietal cortex (Kalaska et al., 1990; Sergio et al., 2005; Hamel-Paquet et al., 2006) supported the view that while MI output correlated better with movement kinetics, parietal cortex operations were more concerned with encoding movement kinematics. Therefore, these last studies were in line with the classical hierarchical model of

cortical control of movement, for which high-order areas, such a parietal cortex, specified movement kinematics, while downstream areas, such as MI, movement kinetics.

In the meanwhile, an emerging perspective was that the encoding of movement kinematics and kinetics were encoded in a parallel fashion in different areas of the parieto-frontal system, also thanks to a recursive signaling sustained by reciprocal cortico-cortical connections (Johnson, et al., 1996; Caminiti, et al., 1996). This view was also supported by the description of different parallel cortico-spinal system originating, beyond MI, from all premotor areas projecting to it (see Dum & Strick, 1991, Lemon, 2008) and, as recently shown, from posterior parietal cortex (Rathelot, et al., 2017; Innocenti, et al., 2018) as well. This perspective received additional support from human fMRI studies (Ehrsson, et al., 2001).

Moreover, a case-report of a parietal patient studied in Battaglia-Mayer's lab (Ferrari-Toniolo, et al., 2014) showed a defective control of the direction of the dynamic hand force application over time, in absence of significant reduction of force magnitude. The results of this study prompted a full reassessment of the relationships between neural activity and dynamic force in posterior parietal cortex of monkeys (Ferrari-Toniolo, et al., 2015). The result was that hand dynamic force and it change over time, but not the amount of force exerted by the subject, are significantly encoded in the activity of cells in macaque parietal area (PFG). Moreover, since PFG is also the parietal node of the mirror system (see Rizzolatti et al. 2014), in Ferrari-Toniolo et al. experiment, cell activity was also studied during trials in which monkeys merely observed on a screen the result of their hand force application, as motion of a visual cursor on the screen. It was therefore possible to determine that the activity of most cells in area PFG was modulated by the hand force necessary to implement the desired target motion, reflecting an inverse model, rather than by the intended motion of the visual cursor (forward model). Since then, different studies have confirmed the crucial involvement of parietal cortex in encoding hand force during grasping (Davare et al., 2007; Neely et a., 2013; Keisker et al., 2010; Intveld et al., 2018). Today, despite 50 years of behavioral neurophysiological studies on the relationships between

cell activity and force in monkeys, only few studies available on the encoding of hand force in PMd (Werner et al., 1991; Hepp-Reymond, et al., 1994; 1999; Xiao et al., 2006), in spite of its direct connections with both MI and the motor output centers of the spinal cortex (see Caminiti et al., 2017). Furthermore, since the discovery of the mirror system (Gallese, et al., 1996; Rizzolatti, et al., 1996), an increasing number of studies has shown action observation-related activity in several areas of the parieto-frontal system, including MI (Tkach, et al., 2007; Dushanova and Donoghue, 2010; Hatsopoulos and Suminski, 2011) and PMd (Cisek & Kalaska, 2004; Tkach et al., 2007). The congruence between action observation- and execution-related activity in PMd has been related to covert mental rehearsal of action, to motor learning and communication, with implications for the development of neurally-controlled prosthetic devices (Suminski et al., 2009). However, it remains to be determined whether PMd cells modulated by action observation also encode motor parameters, such as dynamic hand force, and/or his observable consequences on the action space.

Starting from this background, the aim of the present work is to understand how PMd encodes hand-force and the observation of its output, and how these processes interact.

To this objective, three macaque monkeys were trained in a "hand-force" condition, which required to move a visual cursor on a screen toward eight peripheral targets by exerting a force on an isometric joystick, in absence or presence of an opposing force field. Monkeys were also trained in an "observation" task, in which they observed the result of their action, in the form of motion of a visual cursor on a computer screen. This approach combines in a single experiment isometric action performance and observation of its consequences in the external world, in a way that allows the study of PMd encoding of action parameters by dissociating the representation of inverse and forward models of action, as done in posterior parietal cortex by Ferrai-Toniolo et al. (2015). This also allows a direct comparison of the relative contribute of different parietal and fontal areas in encoding hand force and its change over time in the parieto-frontal system.

MATERIALS AND METHODS

Animals and surgical procedures

Three male rhesus monkeys (*Macaca mulatta*; Monkey 1 (S); body weight 7.5 kg. Monkey 2 (K); body weight 8.5 kg. Monkey 3 (D); body weight 12.3 kg) were used. All surgical procedures were performed under aseptic conditions. The animals were pre-anesthetized with ketamine (10 mg/kg, i.m.) and anesthetized with a mix of oxygen/isoflurane (1%–3% to effect). A circular recording chamber (18 mm inner diameter) was mounted over the dorsal premotor cortex (PMd, area 6), to allow neural recording from a region corresponding to area F2 ((Matelli, Luppino, & Rizzolatti, 1985) (Matelli, Luppino, & Rizzolatti, 1991) (see Fig 1B). At the end of the experiment, for a post-mortem examination, the dura was opened, and reference pins were inserted at known chamber coordinates, to delimitate the recording region and facilitate recognition of the entry point of microelectrode penetrations and their reconstruction relative to key anatomic landmarks, such as the central and the arcuate sulcus.

Animal care, housing, and surgical procedures were in conformity with the European (Directive 63-2010 EU) and the Italian (DL 26-2014) legislative decree on the use of non-human primates in scientific research.

Experimental apparatus, behavioral control, and tasks

During recording session each animal was placed in a darkened, sound-attenuated chamber and seated on a primate chair, with its head fixed in front of a 40-inch monitor (100 Hz, 800×600 resolution, 32-bit color depth; monitor-eye distance 150 cm) and was instructed to control a visual cursor on the screen by applying a force pulse on an isometric joystick (ATI Industrial Automation), which measured the force applied with the hand in two dimensions, with a sampling frequency of 1000 Hz. During the experiment, monkey S and monkey K used the right arm, whereas monkey D used the left arm, while their other arm was gently restrained.

Monkeys were trained in two main tasks: the *Isometric* (*Iso) and Observation* task *(Obs) task.* (see Fig 1A). In addition, during selected recording sessions, Monkey D was exposed, unexpectedly, to a new task condition, *Re-Calibration* (*Re-Cal*; see below for details) which required a change of force output to guide the visual cursor in the desired location, without prior training. Finally, an eye saccade task (*Sac*, Fig.1A) was used as a control condition, to evaluate the influence of eye movement-related signals on the recorded neural activity.

Isometric hand condition (Iso)

In a classical center-out paradigm, a central target [4 degrees of visual angle (DVA) in diameter] and a cursor (0.6 DVA in diameter) were first presented on the screen (see Fig. 1A). The cursor was located in proximity to the central target with a small offset separation from its border, corresponding approximately to 2 DVA. By exerting a force on the joystick (0,8 N), the animal had to move the cursor within the central target, and to keep it there by exerting a constant *static force* for a given control time (center holding time, CHT, 500–600 ms), at the end of which one of eight peripheral visual targets (PT) was presented (8 DVA eccentricity). After a reaction time (RT; upper limit 800 ms), by applying a *dynamic force* for a given time (dynamic force time, DFT, upper limit 2000 ms), the animal moved the cursor from the center to the lighted target and maintained it there for a variable target-holding time (THT, 50–100 ms), which for its short duration reflected the achievement of the action end-point. It is known from oculomotor studies that this epoch rather than reflecting the eye position of the end of a saccade, reflects its recent history (Genovesio, Brunamonti, Giusti, & Ferraina, 2007). The reward, consisting in drops of water or fruit juice, was given if each trial was performed within the pre-specified temporal limits. It is worth stressing that, to move and bring the visual cursor to the target, the animal applied a proper force amount in given directions, in absence of joint displacement. Typically, a force pulse of 1N resulted in a cursor displacement of 2.5 DVA. Therefore, the animal had to increment the hand force exerted on the joystick of ~3.2 N to bring the cursor from the center to the peripheral target (8 DVA eccentricity). In this task, the animals were free to move their eyes without any spatial and temporal constraint. A minimum of 64 trials were collected, in this task condition, since the animals performed at least eight replications in each movement directions.

Observation task (Obs)

Intermingled with the trials of the *Iso* task, in 50% cases *Obs* trials were presented, with temporal structure similar to that of the *Iso* task (see Fig. 1A). During the CHT (500–600 ms), the animal moved its cursor from the offset position inside the central target; a peripheral target (PT) was then presented, and after a variable time, that on average was equal to the RT seen in the *Iso*, a visual cursor was presented and moved toward the PT, and remained within the PT for a variable time (CPT, 50–100 ms). The cursor' motion was similar to that used by the animal in the *Iso* trials. In fact, its trajectories corresponded, after a random selection, to those collected during the execution of isometric task. During the time of cursor's motion (CMT), the animal, who was required to hold its own cursor on the central target for the entire duration of the trial to get its reward, observed the moving cursor, as shown by the analysis of eye movement behavior, which had no restrictions during the *Obs* trials. As in the *Iso* task, a total of a minimum of 64 *Obs* trials were collected during each recording session (8 replications x 8 movement directions).

Recalibration task (Re-Cal)

In 30 sessions, to dissociate the information about the cursor displacement (position and direction) and the amount of force exerted by the animal, we have introduced a variation of the *Iso* task. In this new type of trials (*Re-Cal*), the ratio between cursor's displacement on the screen and the force exerted on the joystick, was reduced of 1/2, so that a force pulse of 1N determined a cursor displacement of 1.25 DVA. The animal was therefore required to recalibrate its hand force output in the force task, to compensate for the unexpected perturbation. After adaptation, the perturbation was removed during a "*Wash-out*" session, to allow the animal to return to its basic pre-perturbation performance (i.e., *Iso* task). In these sessions, the neural activity was recorded in the three consecutive blocks of *Iso*, *Re-Cal* and *Wash-out* trials, each consisting of at least 64 successful trials.

Saccade task (Sac)

To evaluate the influence of eye-related signals on the neural activity recorded during the *Iso*, *Re-Cal*, and *Obs*, a saccadic eye movement task was used as control. The monkeys fixated a white central target for a variable center-holding time (CHT, 700–1000 ms). Then, one out of eight possible peripheral targets was presented at 45° angular interval, on a circle of 8 DVA radius. To obtain a liquid reward, the monkey was required to make a saccade to the target and keep fixation there for a variable eTHT (300–400 ms). Upper limit for eye reaction time (eRT) and movement time (eMT) were both set at 800 ms. In all task conditions, eye movements were sampled (at 220 Hz) through an infrared oculometer (Arrington Research) and stored together with joystick force signals and key events, which were sampled at 1 kHz. The National Institutes of Health-funded software package REX was used to control stimuli presentation and to collect eye movement and hand force data.
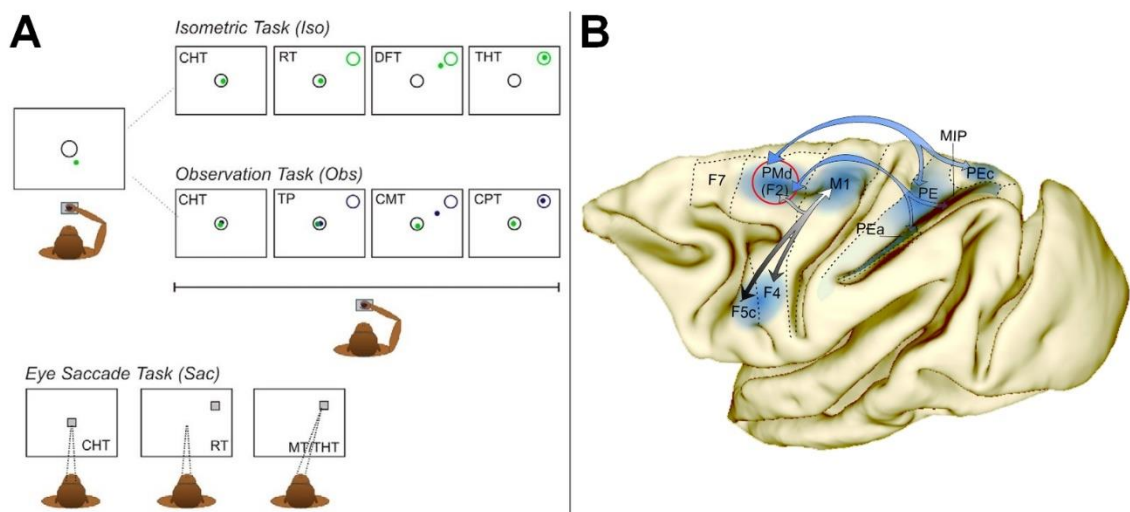

Figure 1. Apparatus, tasks, and recording sites. **A**. The monkey controlled a cursor (green dot) on a screen, by applying a force pulse on an isometric joystick, to perform two types of intermingled trials of the *Iso* and *Obs* tasks. All trials began with the presentation of a circle on the center of the screen (A, leftmost panel). The animal had to move the cursor from its offset position within the central target and keep it there by exerting a static force for a variable CHT. In the *Iso* trials, a peripheral green target was presented in one of eight positions, and within a given RT the monkey had to guide the cursor toward it, by exerting a dynamic force of appropriate magnitude and direction (DFT) and hold it there for a short target holding time (THT). In the *Obs* trials, the animal kept his cursor on the central target, and at the end of the CHT, a peripheral blue target was lighted. The animal was required to observe the movement of a second cursor (blue dot) toward the target, while maintaining his own cursor at the center. In the *Sac* task, the monkey performed saccades to a visual target presented in one of eight locations. The animal used the contralateral arm to the recording chamber. **B**, Recording site in area PMd (F2) of Monkey S, Monkey K and Monkey D (red circle). Arrows indicate the connections of the area of recording with motor cortex, ventral premotor cortex and posterior parietal cortex. F7, rostral dorsal premotor cortex. F2, caudal dorsal premotor

cortex. F5c, the caudal part of the rostral ventral premotor cortex. F4, caudal ventral premotor cortex. M1, primary motor cortex. PEa, PE, PEc, superior parietal lobule. MIP, medial intraparietal cortex.

Behavioral analysis

The force applied by the animal (*subject force*) was measured through an isometric joystick. At the beginning of each trial, an offset was applied to the cursor's position, requiring the subject to exert a force (*static force*) to bring it into the central target, and to keep it there during the CHT. To move the cursor from the center to the peripheral target, the force had to be dynamically changed in amplitude and direction. Therefore, the vector describing the force exerted by the subject on the joystick can be decomposed in a static and a dynamic component, according to the relation: *subject force = static force + dynamic force*.

The instantaneous force change during the cursor motion was defined at each time point as the difference vector between the force at a given 10 ms time bin t and the force at the previous time bin as follows:

$$\text{\textit{instantaneous force change} (t) = \textit{force} (t) – \textit{force} (t – 1)}$$

where "force" can equally represent either the subject force or the dynamic force, being the static force component constant in time. Given that the cursor position on the screen was proportional to the applied force, the instantaneous force change was proportional to the displacement of the cursor between two consecutive time bins and, consequently, to its instantaneous velocity on the screen.

The force signal was low-pass filtered (FIR filter, cut frequency 30 Hz, order 100) and down-sampled to 100 Hz.

The RT was defined as the time elapsing from the presentation of peripheral target to the onset of the cursor's motion, whereas the DFT was defined as the time from the cursor's motion onset to its entry into the peripheral target, thus corresponding to the entire cursor's motion time. The cursor motion onset was determined as the first deviation of cursor velocity exceeding 3 SDs of the signal calculated around target onset (from 50 ms before to 50 ms after target onset time), for at least 90 ms.

Electrophysiological recordings

Neural activity from single cells was recorded extracellularly through a 5 channels electrode matrix (Thomas Recording) equipped with quartz-insulated platinum-tungsten fibers (80 μm diameter, 0.8–2.5 MΩ impedance). Electrodes were equidistantly disposed in a linear array with inter-electrode distance of 0.3 mm and inserted through the intact dura into the cortical tissue. The raw signal was amplified, digitalized, and optically transmitted to a digital signal-processing unit (RA16PA-RX5-2, Tucker-Davis Technologies) where it was stored together with the key events at 24 kHz. The raw signal was also filtered in actual time with a digital biquad filter (0.3–5 kHz), to obtain a threshold-triggered, window-discriminated single unit activity (SUA). SUA data were further discriminated offline.

Analysis of neural data

Single-unit activity.

To characterize the firing rate of a single unit in the different tasks and directions, the spike density function (SDF) during each trial was first calculated. The SDF, obtained by convolving the spike train data with a Gaussian kernel (30 ms width, 1 ms resolution), was then averaged over successive 10 ms time bins, thus obtaining the temporal evolution of the firing frequency with a sampling rate of 100 Hz. The mean firing frequency for the epochs of interest (RT, DFT) was calculated as the averaged SDF across replications during each epoch. A two-way ANOVA (Factor 1: epoch; Factor 2: direction) here referred as ANOVA 'ED' was used to assess significant modulation of cell activity within a particular epoch, relative to CHT ($p < 0.05$ for any factor or for their interaction). A further two-way ANOVA (Factor 1: condition; Factor 2: direction), here referred as ANOVA 'CD', was used to test significant ($p < 0.05$, for Factor 1 or for the interaction) differences of cell activity across different tasks.

Cells were considered as modulated when a statistically significant modulation (2w ANOVA, $p < 0.05$, see above) of the firing rate between the control time (CHT) and at least one epoch of interest (RT, DFT or THT) occurred.

Population activity

The population SDF was obtained by first standardizing each unit's SDF across all task conditions. The average activity and its standard error (SE) across all units was then computed for each bin, thus obtaining the temporal evolution of the standardized population SDF. To compare the population activity across two conditions (e.g., *Iso* vs *Re-Cal*) during epochs of interest, the average value of each unit's standardized SDF was computed. The resulting activities were then compared by means of a two-sample t-test ($p < 0.05$).

Directional tuning of single cells

The directional tuning of cell activity was computed through a nonlinear fitting procedure. A truncated cosine function was fitted into the experimental mean firing rates, calculated during the epochs of interest (e.g., RT, DFT, THT), using the least square method. The fitting model was described by the following directional tuning function as follows:

$$F(d) = \begin{cases} A + B \, \cos(\alpha(d)) & |\alpha| \leq \pi \\ A & |\alpha| > \pi \end{cases}$$

where F is the firing rate (in spikes/sec) as a function of the direction of movement (*d*) expressed in radians. The argument of the cosine function, $\alpha(d) = (d - \text{PD}) \cdot \pi/\text{TW}$, contains two fitting parameters: the preferred direction (PD) expressed in radians, and the tuning width (TW, radians). The other parameters resulting from the fitting procedure (A and B) are linked to the tuning gain (TG) and to the baseline firing rate (*BF*) by the relations: TG = 2B and BF = A - B.

The statistical significance of the directional tuning was assessed using a bootstrap procedure, to test whether the degree of directional bias of the tuning curve could have occurred by chance (Georgopoulos, Kettner, & Schwartz, 1988). The parameter used in this procedure was the tuning strength (TS), defined as the amplitude of the mean vector expressing the firing rate in polar coordinates (Crammond & Kalaska, 1996). This quantity represents the directional bias of the firing rate: TS = 1 identifies a cell that only discharges for movements in one direction, whereas TS = 0 represents a cell with uniform activity across all directions (Batschelet, 1981). A shuffling procedure randomly reassigned single-trial data to different target directions, and the TS was determined from the shuffled data. This step was repeated 1000 times, obtaining a bootstrapped distribution of TS, from which a 95% (one tailed) confidence limit was evaluated. A cell was labeled as directionally- tuned in a specific epoch if the TS value calculated from the original unshuffled data was higher than the computed confidence limit ($p < 0.05$).

Population vector analysis

To study the directional correspondence between the overall population activity and the behavioral output as a function of time, a population vector (PV) analysis was performed. The analysis was performed on the neural and behavioral data from 500 ms before to 500 ms after the cursor's motion onset.

The population vector $\overrightarrow{PV}$ for a given target direction d at a given time bin t, was calculated in standard fashion as follows:

$$\overrightarrow{PV_d}(t) = \sum_i w_d^i(t) \cdot \overrightarrow{PD_i}$$

where $\overrightarrow{PD_i}$ is the preferred direction of the *i-th* cell and $w_d^i(t)$ is its weighted discharge rate during movements toward targets in direction d, at time t. The PDs were obtained from neural activity collected during DFT of *Iso*, *Re-Cal*, and *Wash-out* tasks.

The weight function for a given cell was defined as follows:

$$w_d(t) = \frac{FR_d(t) - FR_{avg}(t)}{R(t)}$$

where $FR_d(t)$ is the firing rate of that cell at time t for movements toward direction d, $FR_{avg}(t)$ is its discharge rate averaged over all directions at each time bin (t), and R(t) = (max($FR_d(t)$) - min($FR_d(t)$)/2 represents the half-range of its activity across directions (Georgopoulos, Kettner, & Schwartz, 1988). By using this weight function, the contribution of each cell to the population vector is normalized, ranging from - 1 to 1 for symmetrically distributed firing rates.

The population of cells used to compute the PV included only the units that showed a significant directional tuning (see above) during the DFT of the center-out task.

Decoded trajectories of cursor motion

A neural representation of the applied force in time, hence of the resulting cursor trajectory, based on the information encoded by the population vector, was constructed following two different hypotheses. As a first hypothesis, the $\overrightarrow{PV}$ was assumed to encode the dynamic force, that is, the force to be exerted by the animal to bring the cursor from the center to the periphery. Therefore, a representation of the applied force at each time bin was obtained by placing each instantaneous population vector $\overrightarrow{PV}_{(t)}$ at the center of the workspace. As a second hypothesis, the $\overrightarrow{PV}$ was assumed to encode the instantaneous force change (i.e., the infinitesimal increment of force applied at any given time). In this case, a representation of the predicted force exerted on the joystick was obtained by connecting tip-to-tail all the $\overrightarrow{PV}_{(t)}$, with t starting at the movement onset time (Georgopoulos, Kettner, & Schwartz, 1988). To quantify the similarity between the "actual" cursor trajectory resulting from animal force application and the "decoded" trajectory reconstructed from the PV analysis, a vector time series were first constructed from each of the trajectories to be compared, with elements representing the displacement between two consecutive points.

RESULTS

Neural activity related to dynamic hand force production and observation the resultant visual cursor's motion

The electrical signs of the neural activity of 643 cells was recorded from area PMd from three macaque brains, and studied in three different tasks: *Iso, Obs* and *Sac*. The proportion of cells with neural activity significantly modulated and directionally tuned in the above-mentioned tasks is shown in Figure 2.
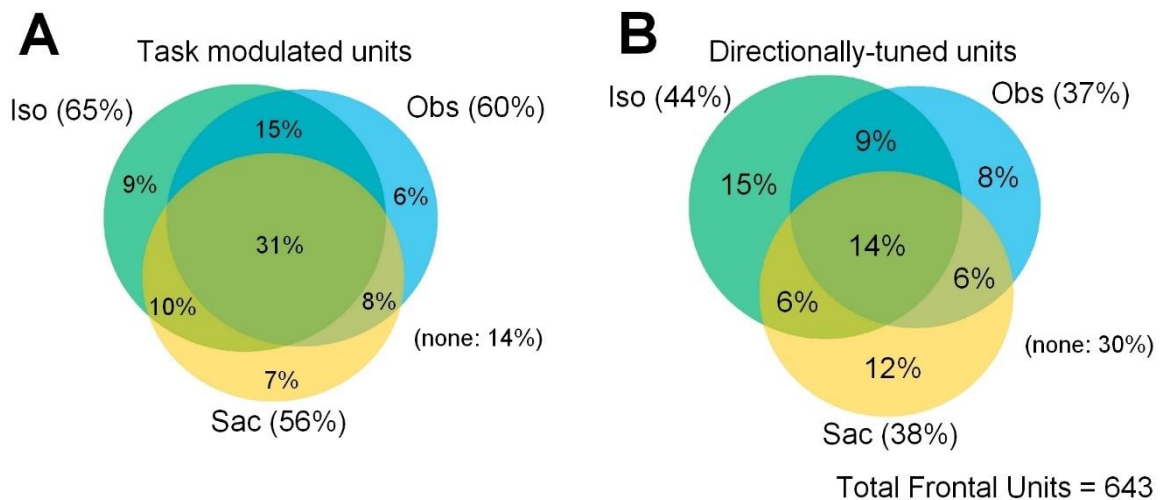

Figure 2. Venn diagrams showing the percentages of cells significantly modulated (A) and directionally tuned (B) in the isometric force (*Iso*), observation (*Obs*) and Eye Saccade (*Sac*) tasks. The "none" group shows the proportion of cells that were not modulated (A) or directionally tuned (B) in any condition. In **A**, modulation was assessed through a 2w ANOVA ($p < 0.05$), while directional tuning was statically evaluated through a bootstrap technique (see Methods for details)

It can be seen that a similar proportion of cells was modulated in *Iso* (65%) and *Obs* (60%) tasks (Figure 2A). Furthermore, we found that many cells (56%) were modulated in the *Sac* task. Similar results were obtained from the analysis of the directional modulation of cell activity (Figure 2B).

Since we were interested in studying the neural encoding of hand force, the following analyses were performed on a dataset (n = 283) obtained by excluding saccadic-related cells.

Figure 3 illustrates the activity of three typical task-related neurons (Fig. 3 A, B, C, upper panels) that are strongly representative of our dataset.
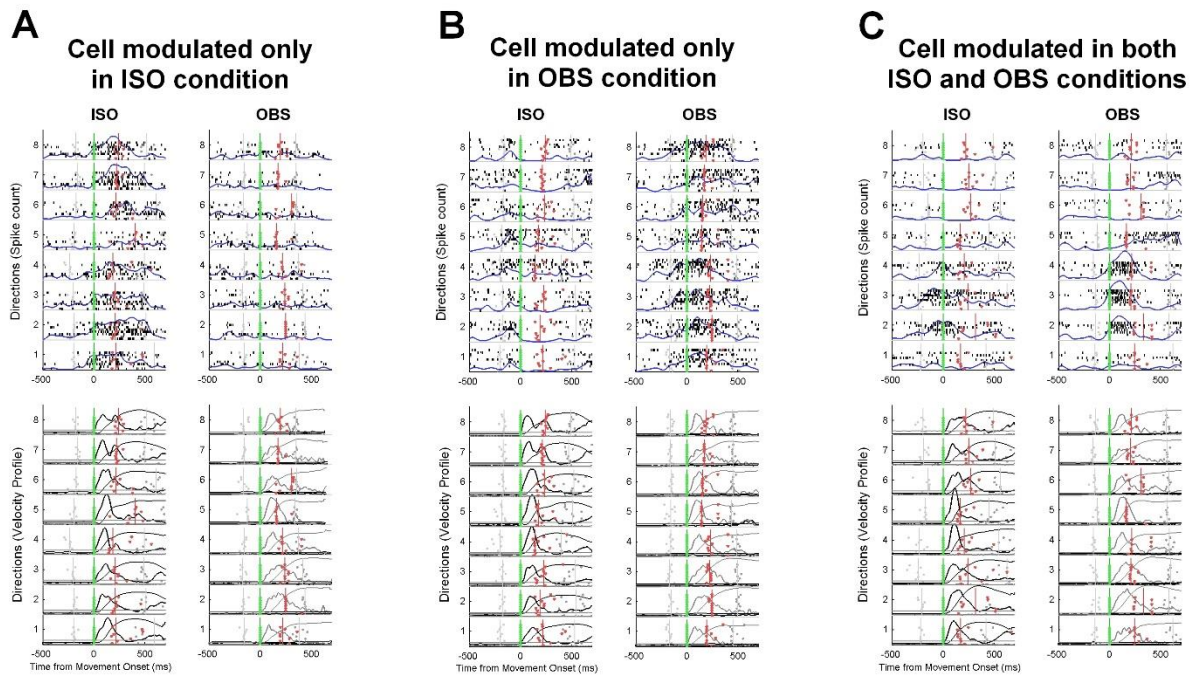
Figure 3. Neural activity of three typical cells recorded from area PMd during the *Iso* and *Obs* tasks. A, B, C. Examples of cells significantly modulated (ANOVA, $p < 0.05$) only in the *Iso* task (A), only in the *Obs* task (B), or in both conditions (C). In the upper panels, the neural activity is displayed in the form of raster plots with superimposed SDFs in the eight different directions of the task adopted. In the *Iso* and *Obs* tasks, activity is aligned to the onset of hand ramp force (0 ms; green vertical line). Gray vertical lines before and after the onset of DFT indicate target presentation and end of THT, respectively, while the red vertical line indicates cursor's entry on the target. The lower panels display the behavioral data collected during recording the cell activity shown in upper panels: dynamic force pulses (thin curves), force velocity profile (thick cur\ves) during the *Iso* and *Obs* tasks.

Figures 3A and 3B show the activity of two typical cells significantly modulated in only one of the two behavioral conditions. The *Iso*-related cell (Fig. 3A) was significantly modulated during the DFT and during the static holding of the cursor on the peripheral target (ANOVA 'ED', $p_{epoch} < 0.001$, ANOVA 'CD', $p_{condition} < 0.001$) and not during the *Obs* condition (ANOVA 'ED', $p_{epoch} = 0.418$). The *Obs*-related cells (Fig. 3B) was significantly modulated during the DFT (ANOVA 'ED', $p_{epoch} < 0.001$, ANOVA 'CD', $p_{condition} < 0.001$) but not during the *Iso* condition (ANOVA 'ED', $p_{epoch} = 0.206$). However, the majority of the cells of our dataset was not modulated exclusively in one task (Fig. 2). In Fig. 3C we report the activity of an example cell with significant modulation and directional tuning in both *Iso* and *Obs* tasks, particularly during DFT epoch (*Iso* condition: ANOVA 'ED', $p_{epoch} < 0.05$, ANOVA 'CD', $p_{condition} < 0.05$; *Obs* condition: ANOVA 'ED', $p_{epoch} < 0.001$, ANOVA 'CD', $p_{condition} < 0.01$). It is worth noticing, however, that this cell modulation and directional tuning, in the *Iso* task appeared, after the Target Onset (Ton), i.e. during the reaction-time (RT). This pre-movement activity

present in the *Iso* condition, disappeared when the animal was instructed to only observe the simulated motion of the visual cursor (i.e. *Obs* condition).

We then analyzed the temporal evolution of the neural activity in the Iso and Obs task, at population level. To this aim we computed the population SDF, by averaging the SDFs of the cells belonging to each of the three datasets (Monkey D, monkey S, Monkey K). We found that in all animals, the population activity recorded in the *Iso* task was not significantly different (two-sample *t* test; $p < 0.05$) to that studied during the *Obs* task (Fig. 4). This was true for the entire duration of the tasks, namely during the RT, DFT and THT.
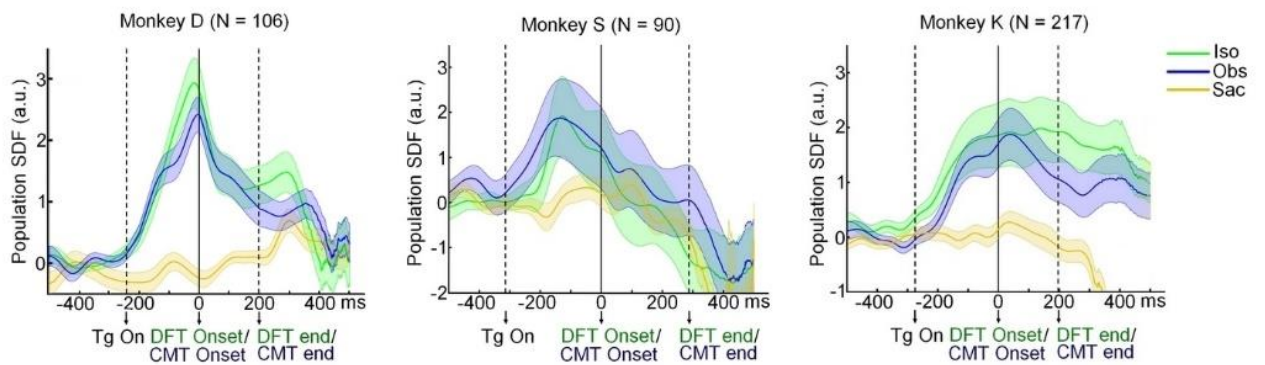

Figure 4. Mean standardized population SDF (±SE) relative to the *Iso* (green), *Obs* (blue), and *Sac* (yellow) tasks in the three monkeys (N, number of cells). Neural activity is aligned to the onset of ramp force.

Therefore, even if the two behavioral conditions differed considerably, the population activity during the DFT was virtually identical to that of the *Obs* condition, in which the monkeys had just to observe the movement of a cursor while exerting a small static force to keep the cursor in the central target of the screen.

Modulation of dynamic hand force by changing the force field: adaptation to a new task dynamics

The activity of a group of 106 cells (selection based on firing rate > 10 Hz) was studied in a task which required the application of a different amount of force to bring the cursor from the center to the peripheral target (Fig. 5A). The cell activity was therefore studied in a sequence of three blocks, characterized by different values of the 'force scaling factor', representing the ratio between the force to be applied and the cursor displacement. The session started with a block of 64 regular *Iso* trials, at the end of which the animal had to perform the isometric task

in a new force condition, referred as *Re-Cal*, during which the new value of the force scaling factor, imposed to the animal an unexpected remapping of the force output on the cursor's motion. The monkey had to readjust the hand force exerted on the joystick, by doubling it, in order to bring the cursor to the desired location.
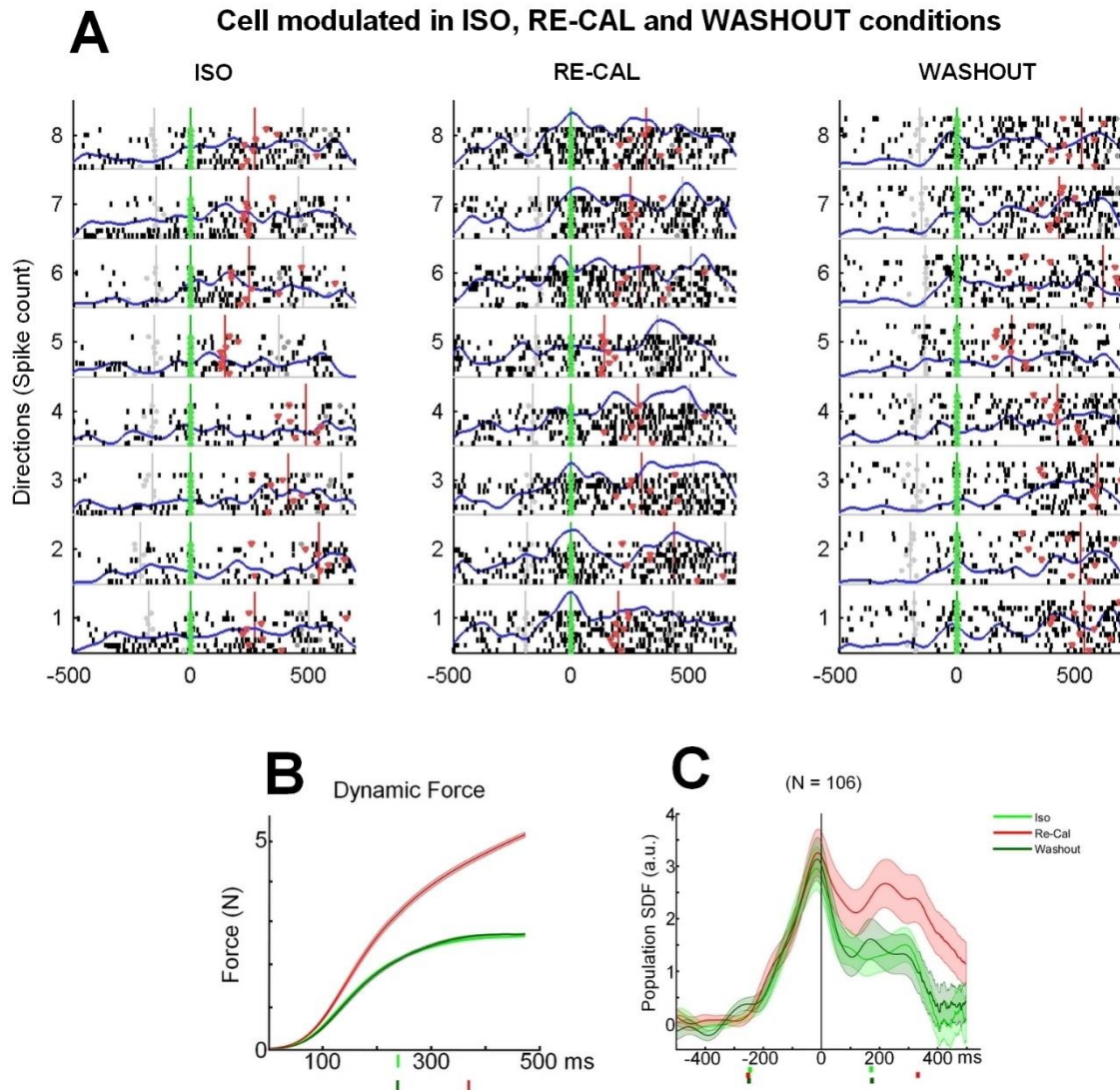

Figure 5. Effects of force recalibration on premotor cells. *A*, Neural activity of a typical cell recorded from area PMd during the *Iso* (FR = 13,64 spikes/sec), *Re-Cal* (FR = 34,27 spikes/sec), and *Wash-out* (FR = 9,88 spikes/sec) task, displayed in the form of raster plots (dots), with the SDFs (blue curves) superimposed, in eight directions. Activity is aligned to the onset of ramp force (0 ms; green vertical line). Gray vertical lines before and after the onset of DFT indicate target presentation and the end of THT, respectively, while red vertical line indicates cursor's entry on the target. *B*, Mean (±SE) amount of force exerted by the animal from the onset of its application (0 ms) to bring the cursor from the center to the peripheral target in the three tasks. The *Iso* and *Wash-out* conditions are represented in light green and dark green, respectively; the *Re-Cal* condition in red. **C**, Mean standardized population SDFs (continuous curves) and relative SE (shaded area) from cells of monkey D (*N* = 106). The activity is aligned to onset of force application (0 ms). The dots on x-axis before the onset of force (0 ms) represent the

mean time of target presentation. The dots after the onset of force (0 ms) represent the mean time of cursor's arrival at the peripheral target.

The monkey adapted rapidly to the new force condition and after having executed a block of 64 successful *Re-Cal* trials, the activity was then re-tested in a condition, here referred as "*Wash-out*", identical to the *Iso* task. In this block, the perturbation was removed, to allow the animal to return to the basic pre-perturbation condition of the *Iso* task (Fig. 5B). As it can be seen in a typical cell shown in Figure 5A (associated animal's behavior reported in Figure 5B), during the *Re-Cal* task, the firing rate of cell increased significantly with respect to the *Iso* task and returned to the original level when retested in the *Wash-out* session. The first change resulted in a significant increase of the mean firing rate (2-way ANOVA $pC < 0.01$) during the *Re-Cal* condition, occurring in the DFT. In the *Wash-out* condition, instead, this cell significantly reduced its firing rate (2-way ANOVA $pC < 0.01$). The firing rate of this cell during the DFT did not significantly differed between *Iso* and *Wash-out* (2-way ANOVA, $pC = 0.082$ and interaction factor: condition direction, $pCD = 0.149$).

Significant changes of cell activity during force-cursor remapping condition (*Re-Cal*), with respect to the *Iso* task, similar to those described in the example reported above, were observed during the DFT in 68 out of 106 (64%) cells (2-way ANOVA; Factor 1: condition, $pC < 0.05$ and/or interaction factor: condition x direction, $pCD < 0.05$). Most of these cells, increased their firing rate when exposed to *Re-Cal* condition (60%, 41/68). In this group, the neural activity of 36% (15/41), collected during the *Re-Cal* trials, did not change during the *Wash-out* (2-way ANOVA; Factor 1: condition, $pC > 0.05$ and interaction factor: condition direction, $pCD > 0.05$), as if neural response retained memory of the new force-field exposure in the previous trials. However, most cells (53%, 22/41) significantly decreased their firing rate when tested in the *Wash-out* condition. Furthermore, only a very small amount of cells (9%) increased their firing rate across this task condition.

In order to determine how these changes were reflected in the whole population, we calculated the population SDF separately for each behavioral condition of the Task (*Iso, Re-Cal* and *Wash-out*). The results of the three population SDFs aligned to the dynamic force onset are shown in figure 5C, which displays a clear pattern of neural activity which reflect the changes in the dynamic force exerted on the joystick. Statistically significant differences (1-way ANOVA, Factor: condition, $p < 0.05$ and Bonferroni post-hoc test: *Iso* vs *Re-Cal* $p = 0,014$; *Re-Cal* vs *Iso*, $p = 0.049$; *Iso* vs *Wash-out*, $p = 0.89$) were observed during the DFT, characterized by a new dynamical that required an increased force to guide the cursor towards the target, and THT,

during which the force had to be maintained constant, in order to keep the cursor in its endpoint. These differences were absent in the RT, during which the task imposed only the application of a static, even though different, force. Therefore, on premotor cells the remapping process was not reflected during the planning phase of the upcoming action.

Directionally-tuned cells in PMd

To further investigate the coding of force in PMd cells, we studied their directional tuning properties, focusing on the same datasets used for the previous analysis on force recalibration (total number of cells, n=106). In this task condition we also found the highest number of cells with statistically significant directional tuning. This was found only during DFT, in which their proportion was higher in *Re-Cal* (49%) condition, as compared to *Iso* (*25%*) and *Wash*-out (27,30%) task, and in the THT (*Iso*, 26,40%; *Re-Cal, 42%; Wash-out, 32%,* see Table 1). This is also shown by the rose diagrams in Figure 6A, that document a clear expansion in the proportion of PMd cells directionally-tuned in the above conditions and epochs.

Table 1. Number and percentage of cells with significant directional-tuning in Iso, Re-Cal and Wash-out tasks

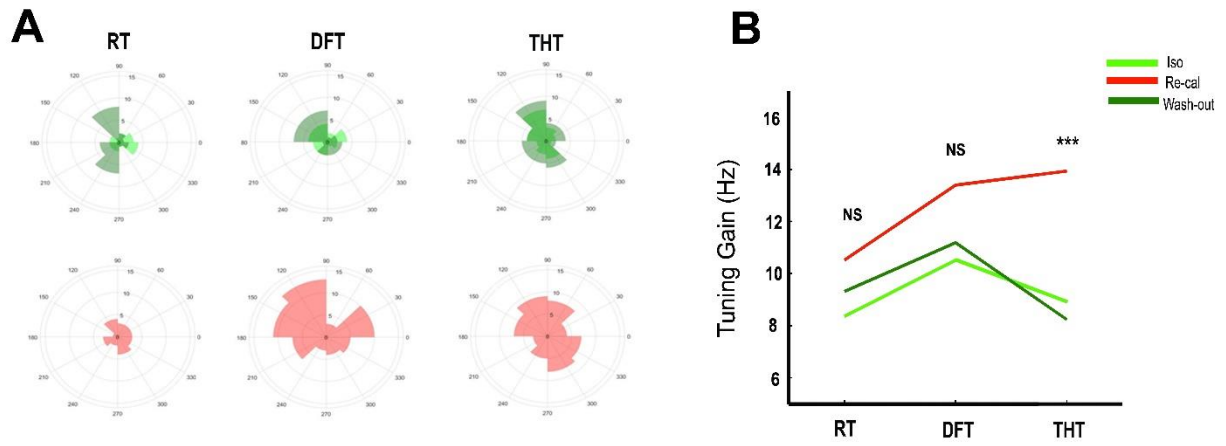| Epoch	Number of cells		
	Iso	*Re-Cal*	*Wash-out*
RT	22/106 (20%)	26/106 (24%)	28/106 (26,4%)
DFT	27/106 (25%)	52/106 (49%)	29/106 (27,3%)
THT	28/106 (26,4%)	45/106 (42%)	35/106 (32%)

Figure 6. Directional properties of cells in *Re-Cal* task. **A**, polar histogram showing the number of cells with a statistically significant directional tuning (bootstrap, $p < 0.05$) for each epoch and task condition. **B**, Tuning Gain, calculated for each epoch and task condition with reported statistic (paired t-test: *, < 0.05, **, < 0.01, ***, 0,001).

Study of the directional properties during perturbation and post-perturbation time

To deepen the description of the properties of frontal neurons exposed to the change in force condition, we evaluated how the force re-calibration affected the tuning properties of PMd cells, by studying both the shift of the preferred direction (PD) and the depth of modulation of the tuning curve (Tuning Gain, TG).

First, we evaluated the shift of their PDs, either when the animal was exposed to the perturbation (*Re-Cal*) and when this was removed (*Wash-out*).

After the change of force conditions, we did not find a significant shift (Watson-Williams for circular data, $p = 0.63$) of cell PDs at a population level. The net shift was rather low but the magnitude of the shift, obtained by calculating the absolute value of the shift of preferred direction for each cell considered and by mediating each cell value, was higher than the shift observed in the *Wash-out* condition. The observation that after the *Wash-out* of the force field, the preferred direction tended to return to the orientation observed in the *Iso,* is also confirmed by the lower magnitude of the PD shift between *Iso/Wash-out* (14,34°) than between *Iso/Re-Cal* (22,39°) conditions, although this difference did not resulted significant (Watson-Williams for circular data: difference$_{Iso-ReCal}$ vs difference$_{ReCal-Washout}$, $p = 0.794$; difference$_{Iso-Washout}$ vs difference$_{Iso-ReCal}$, $p = 0.238$; difference$_{Iso-Washout}$ vs difference$_{ReCal-Washout}$, $p = 0.139$).

Furthermore, the lack of a net shift of PD after perturbation could depend on the type of force field adopted in our experiment, that did not impose any directional bias to the cursor's motion, but rather a modification of the force amplitude. However, by subdividing the original

population in two sub-populations, for each of them we found an important variation from the preferred directions observed in the *Iso* condition.

We also investigated the depth of tuning modulation of the cells in all three behavioral conditions for each of the three task epochs. Figure 6B shows that directionally-tuned cells during the execution time of the *Re-Calibration* condition display an increased tuning gain, as compared to the *Iso* condition. Notably, these differences were only statistically significant for the THT (1-way ANOVA, Factor: condition, $p = 0.0011$), while for DFT there was only a tendency towards significance (1-way ANOVA, Factor: condition, $p = 0.061$). This result suggests that the total force modulation needed was stronger at the end of the isometric action, to stop the cursor's motion, rather than during its motion.

Force output modulation in two different population of cells

Given the numerical relevance of PMd cells modulated in the *Obs* task, we decided to study the role of different cells populations in the force recalibration process. For this, we divided the 106 cells considered for all above analyses of directional properties in two groups: *a)* a first one was formed by cells modulated (ANOVA, $p < 0.05$) during the DFT of the *Iso* condition (without any requirement on the modulation in the *Obs* task); *b)* a second group included cells modulated during the cursor's motion time of the *Obs* trials but not in the *Iso* condition. We noticed that the *Iso*-modulated cells showed a significant decrease of their normalized activity with respect to that recorded during the *Obs* condition (Fig. 7A), while the second group on the contrary where more strongly modulated by the *Obs* task, with respect to the *Iso* one. Therefore, we were interested in analyzing which was the role of each of the two subsets of cells in the 'recalibration' process, tested by perturbing the force field. To this scope, we studied the population SDFs of both groups in the *Iso, Re-Cal* and *Wash-out* for the two groups separately (Fig. 7C, D). For both groups, the neural activity in the *Re-Calibration* condition was studied by analyzing the respective population SDFs (Fig. 7). While the cells of group *a)*, which was modulated in the *Iso* task (Figure 7A), changed their response (paired t-test, $p < 0.05$), thus reflecting the increase in the amount of force imposed by the force recalibration (Figure 7C), those of group *b)* (Figure 7B) did not significantly change their activity profile during force perturbation, therefore were not affected by the change in task dynamics (paired t-test, $p > 0.05$; Fig. 7D),
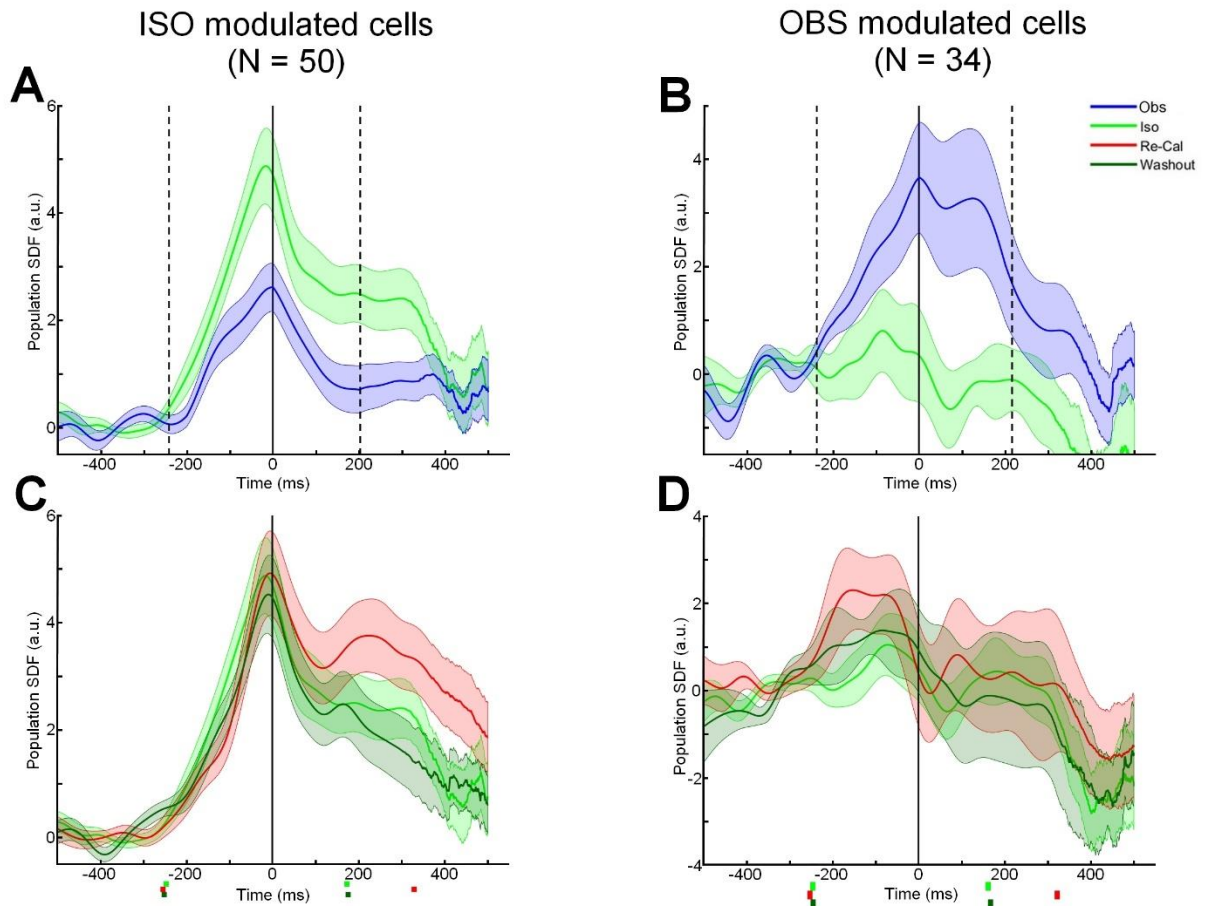
Figure 7. Mean standardized population SDFs (continuous curves) and their SE (shaded area) from two subsets of cells in monkey D (N, number of units). Neural activity is aligned to onset of force application (0 ms). The markers before the onset of force (0 ms) represent the mean time of target presentation. The markers after the onset of force (0 ms) represent the mean time of the cursor's arrival at the peripheral target. **A**, mean population SDF from cells significantly modulated in *Iso* task ($p < 0.05$) and whose firing frequency was significantly ($p < 0.05$) higher in the *Iso* task (green) than in the *Obs* task (blue). **B,** mean population SDF from cells significantly modulated in *Obs* task ($p < 0.05$) and whose firing frequency was significantly ($p < 0.05$) higher in the *Obs* task (blue) than in the *Iso* task (green). **C**, Mean population SDF from cells significantly modulated in *Iso* task ($p < 0.05$) and tested in *Iso* (green), *Re-Cal* (red) and *Wash-out* (dark green) conditions. **D**, mean population SDF from cells significantly modulated in *Obs* task ($p < 0.05$) and tested in *Iso* (green), *Re-Cal* (red) and *Wash-out* (dark green) conditions.

Population coding of hand force output and cursor's kinematics

The neural representation of the behavioral output as a function of time was studied by comparing the temporal evolution of the instantaneous PV (computed at 10 ms time bins) with both the evolution of the instantaneous force change (see Materials and Methods), a time-varying force vector controlled in the *Iso* task, and the kinematics of the cursor during the *Obs* task, in absence of any hand force change. As shown in previous studies of motor

(Georgopoulos, Ashe, Smyrnis, & Taira, 1992) and parietal (Ferrari-Toniolo, Visco-Comandini, Papazachariadis, Caminiti, & Battaglia-Mayer, 2015) cortex, also in PMd the PV predicts the instantaneous force changes over time. In fact, we were able to reconstruct the cursor's motion trajectory, i.e., the "decoded trajectory", by placing tip-to tail the instantaneous PVs computed from the activity of premotor cells in each target direction. For this purpose, we divided the cells in two distinct groups, those with significant preferred direction (PD, see Materials and Methods) in *Iso* task (Figure 8A1, B1, C1), and those that presented a PD in *Obs* task (Figure 8A2, B2, C2). Consistent with the previous analysis of the population SDFs, the cells modulated in the *Sac* task were not included.
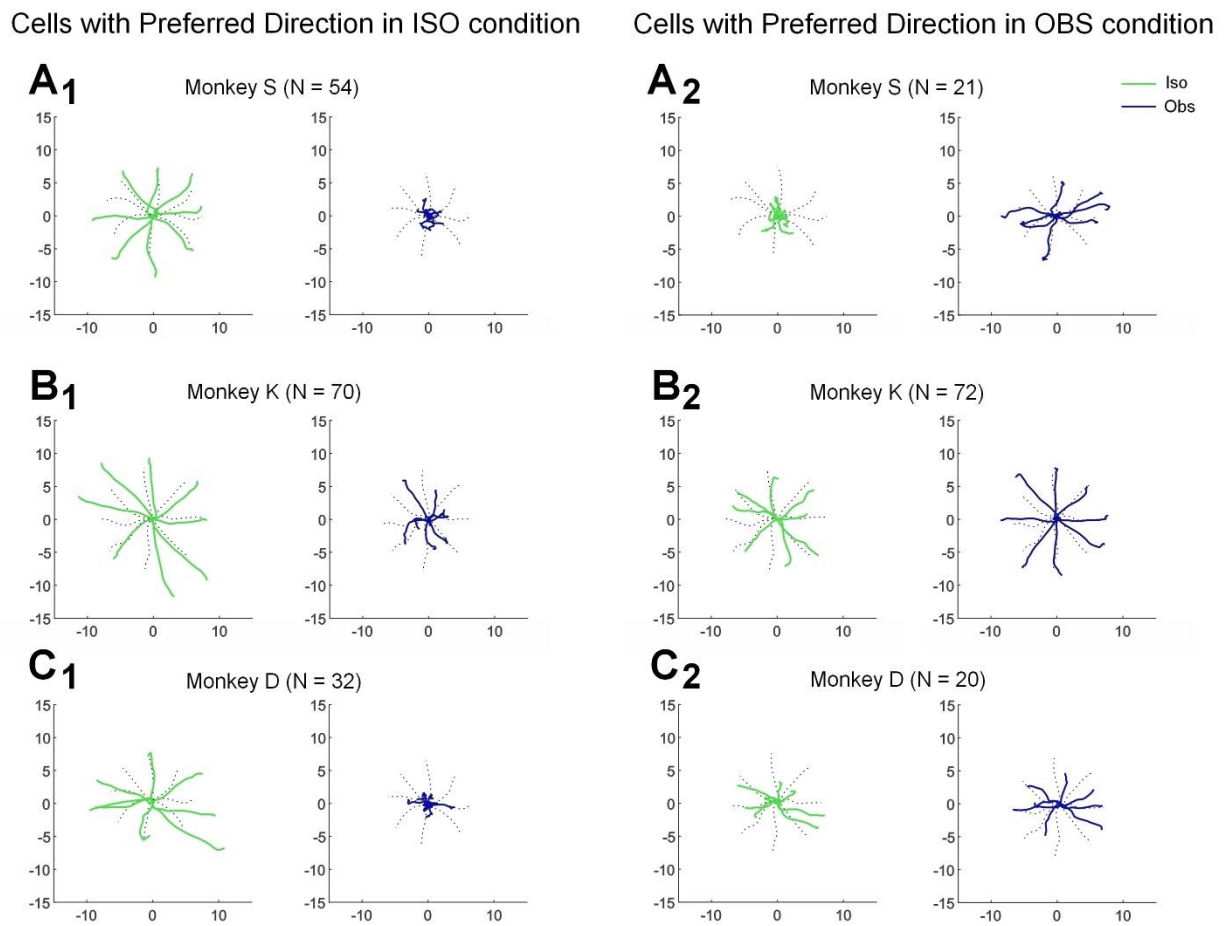

Figure 8. Population vectors and decoded trajectories of cursor motion. Decoded trajectory (thick curve) of the cursor's motion toward the eight target directions, as predicted by the "instantaneous force change" encoding hypothesis, therefore obtained by connecting tip-to-tail all the PVs computed at each time bin from the activity recorded during the *Iso* (green) and *Obs* (blue) tasks. Gray dotted lines indicate mean actual cursor's trajectories. **A1**, Monkeys S, cells with PD in *Iso* task. **A2**, Monkeys S, cells with PD in *Obs* task. **B1**, Monkeys K, cells with PD in *Iso* task. **B2**, Monkeys K, cells with PD in *Obs* task. **C1**, Monkeys D, cells with PD in *Iso* task. **C2**, Monkeys D, cells with PD in *Obs* task.

The results (Figure 8) show that the decoded trajectory of the cursor's motion resulting from force application was predicted with high fidelity in the *Iso* condition (Figure 8A1, B1, C1, green lines) by cells directionally-tuned in *Iso* task of the three monkeys. The temporal evolution of the PV computed through the neural activity recorded during the *Obs* task (Figure 8A1, B1, C1, blue lines) of these cells did not predict the cursor motion associated to this task condition. Indeed, the trajectories were not reconstructed in monkey S (Figure 8A1) and Monkey D (Figure 8C1), while in monkey K they were poorly reconstructed (Figure 8B1). This reflects the scarce influence of this parameter on the activity of this group of cells in the absence of any force production.

Concerning the cells with PD in *Obs* task, the results show that, the trajectories are better reconstructed in the *Obs* condition in the three monkeys (Figure 8A2, B2, C2, blue lines), with respect to the Iso condition. In this case, a variable accuracy of the trajectory prediction has been observed (Figure 8A2, B2, C2, green lines). Indeed, in Monkey S (Figure 8A2) the trajectories are not reconstructed, in monkey D (Figure 8C2) they are poorly reconstructed, while in Monkey K the decoded trajectories are more accurate. Interestingly, the monkey with higher fidelity to behavioral output in both groups of cells (i.e. monkey K, Figure 8B1, B2), is the monkey that also presents the higher percentage of cells with PD in both the *Iso* and *Obs* tasks (See Table 2), therefore with similar tuning properties across task conditions.

Table 2. Number of cells used in PV analysis

Monkey	Cells with PD in Iso	Cells with PD in Obs	Cells with PD in Iso and Obs
S	54/65 (83%)	21/65 (32%)	10/65 (15%)
K	70/107 (65%)	72/107 (67%)	35/107 (33%)
D	32/44 (73%)	20/44 (46%)	8/44 (18%)

Encoding the force determining the desired cursor motion or the intended cursor motion?

The final crucial question of this study was to determine whether cell activity in the task studied encoded the force necessary ti implement the desired cursor motion, thus reflection and inverse model, or rather the intended cursor motion, as in forward models.

To address this issue, the PV analysis was repeated to compare the trajectories decoded from neural activity recorded under different force outputs (*Iso, Re-Cal, Wash-out*). In fact, if cell

activity reflects the force output, it can be expected that the length of the PVs(t) in the *Re-Cal* condition, and consequently the length of the decoded trajectories, would be approximately twice as long as that associated to the *Iso* and *Wash-out* tasks. On the contrary, the PV would reflect the intended cursor motion.
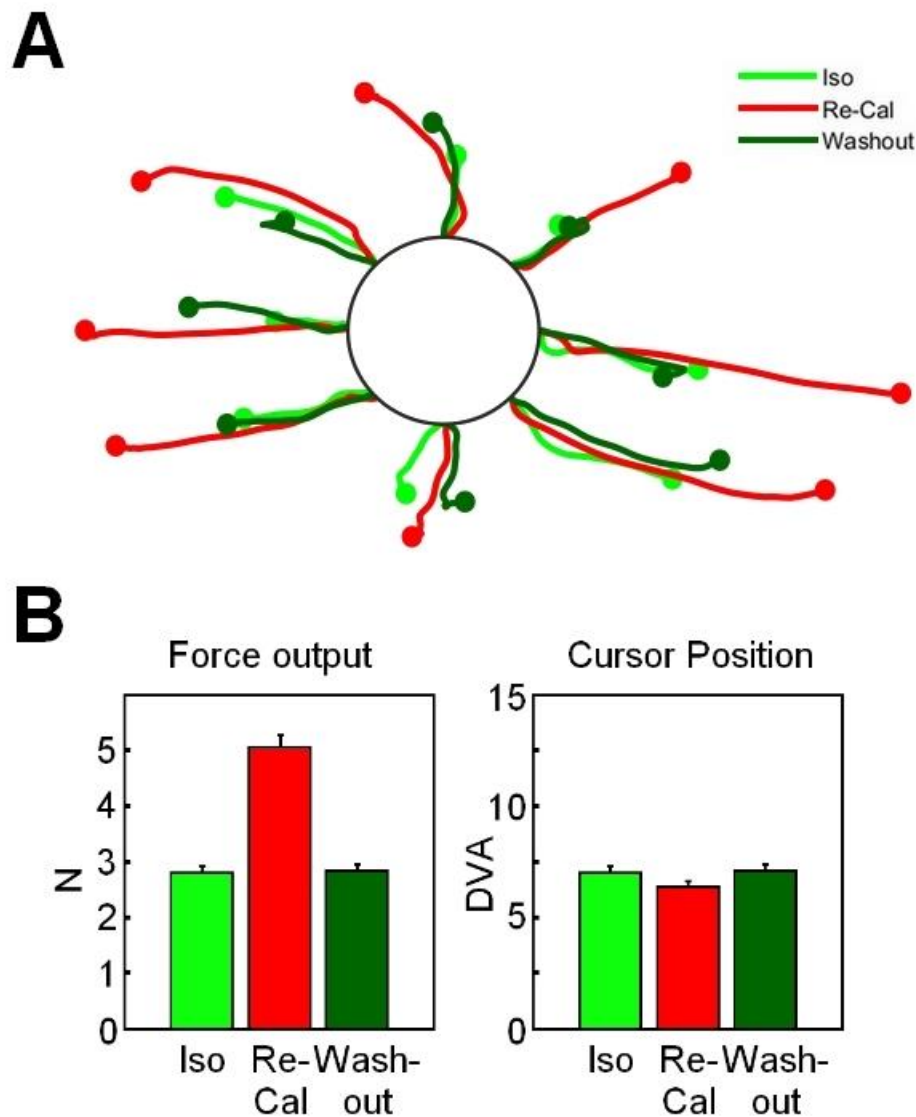

Figure 9. Decoded trajectory and output force. **A**, Decoded trajectories in the eight directions of cursor motion obtained by using the PVs computed for different task conditions (green represents Iso; red represents Re-Cal: dark green represents Wash-out), characterized by different force modulations by the animal, as to bring the cursor from the center to the peripheral target. Trajectories are plotted from the DFT onset to the time the cursor enters the peripheral target (filled circles), by using only cells with significant directional tuning in each task. **B**, Average (±SE) values of force output (in Newton) on the left, and cursor position (distance of the cursor from the central starting position, DVA) on the right, measured at the end of DFT.

Figure 9A shows that in the *Re-Cal* condition, the length of the neural trajectories increases significantly, to return similar to that of the *Iso* task, after the *Wash-out* session, when the force output returned identical to that of the *Iso* task. Furthermore, by plotting the magnitude of exerted force, and the cursor position at the end of DFT across conditions (Fig. 9B), we can conclude that, in these cells, the PV predicts the force variations better than the intended cursor motion on the screen.

DISCUSSION

The goal of this study was to assess the role of PMd in the cortical network encoding hand force, in addition to its well-known role in the control of limb kinematics (Caminiti, Johnson, Galli, Ferraina, & Burnod, 1991). For this reason, we studied the neural activity of a large population of premotor cells in different behavioral tasks. These were aimed at dissociating action kinematics from kinetics and at assessing the relationships between the hand force-related activity and the observation-related activity elicited when the animals observed in play-back the consequences of their hand force output, as motion of a visual cursor on the screen.

Activity of hand force-related cells under different force conditions

Most PMd cells were modulated and directionally-tuned during the time of dynamic force application the *Iso* task. The modulation of neural activity started with varying latencies after the presentation of the visual target, therefore during the RT, reached its peak close to the onset of the dynamic force, that is action onset, and then slowly returned to the baseline. Thus, in many instances cell activity could have been related to the intended direction of force application or to the desired trajectory of the resulting cursor motion.

To determine whether cell activity was truly related to force output, in the *Re-Cal* condition the force/cursor displacement relationships were changed in such a way that the monkeys had to double the amount of force exerted on the joystick to compensate for such change and successfully bring the cursor to the target, as if force was applied against an opposing load. Under these conditions cell activity in a large fraction PMd cells changed significantly, in most instance by enhancing the firing rate, which remained higher than *Iso* condition during the time of force change. In a similar fashion, most cells' preferred direction changed, or even emerged during this time, when the cell was not directionally-tuned in the *Iso* task. Thus, under the new force field conditions, both cells modulation and the direction tuning changed. Finally, these premotor neurons responded to the increased force output by also increasing the power and precision of the directional tuning of cells.

During the *Wash-out* condition, when the force/cursor displacement relationships returned identical to those of the *Iso* task, cells activity in PMd returned to the level of the pre-perturbation conditions.

Encoding the hand force causing the desired cursor motion or the intended cursor trajectory?

The final crucial question of this study concerning encoding of force was to determine whether cell activity in the task studied encoded the force necessary to implement the desired cursor motion, thus reflecting and inverse model, or rather the intended cursor trajectory, as in forward models. To address this issue at the population level, the PV analysis was repeated to compare the trajectories decoded from neural activity under different force outputs (*Iso, Re-Cal, Wash-out*). We reasoned that if cell activity reflected the force output, one could expect that the length of the time-varying population vector in the *Re-Cal* condition, and consequently the length of the decoded trajectories, would be approximately twice as long as that associated to the *Iso* and *Wash-out* conditions. On the contrary, the population output would reflect the intended cursor motion. Consistent with the results obtained at single cell level, we found that the length of the decoded trajectories in *Re-Cal* conditions increased as expected, relative to the *Iso* task, and then returned to the baseline when the new force-field was washed-out. This suggest the cells population output reflects an inverse model that specifies the force necessary to implement the cursor motion appropriate to bring it to the target.

These changes of neural activity across *Iso*, *Re-cal* and *Wash-out* conditions can be interpreted as a neural correlate of motor adaptation to changed task dynamics, that is for rapid error corrections that return behavior to baseline performance (Shmuelof & Krakauer, 2011). They are similar to the data gained in dorsal and ventral premotor cortex from force-field adaptation experiments based on arm movement (Xiao et al., 2006). In the latter study the majority of cell were responsive to changes of the force-field, by changing their PD and/or firing rate, but these cells did not preserve these modifications at the end of the *Wash-out* condition. Thus, there seem to be a common mechanisms of force hand force encoding and response to unexpected modifications of the dynamics of the action space across dorsal and ventral premotor cortex, that reflect an adaptation rather than a learning process.

As compared to the mechanisms of force encoding in posterior parietal cortex under identical task conditions, (Ferrari-Toniolo, Visco-Comandini, Papazachariadis, Caminiti, & Battaglia-Mayer, 2015), an important difference is that, although in the latter neural activity changed in response to the new force field, as in PMd, in parietal cortex at the end of a "*wash-out*" session cell and population activity did not return to the pre-perturbation conditions, thus retained memory of the new learned association, probably at the service of predictive control of future hand force application. Therefore, in such a case a learning process might have occurred.

Furthermore, although the neural hallmarks of motor learning and plasticity were apparently not represented in our results, we observed an intriguing phenomenon which might represent a way to face unexpected change in task dynamics. Indeed, despite after removal of the perturbation of the force field PMd neural activity returned to the level typical of the pre-perturbation condition, at the end of the *Wash-out* session we found an increase in the number of cells recruited in the DFT, as compared to pre-perturbation conditions, as well as a significant shift of cells PD during *Wash-out,* as compared to baseline (*Iso*), even if this shift was less pronounced than in the *Re-Cal* condition.

Altogether these results suggest that at the transition between *Iso*, *Re-cal*, and *Wash-out* conditions, that is across conditions that require exerting an isometric hand force, recalibrating the force output to face an unexpected force field change, returning to the baseline condition after its wash-out, a potential dynamic re-arrangement of the PMd neural assembly underlying these processes occurred, since the assembly size expanded by increased the number of its constituent cells, now endowed with increased directional power and precision, then a reshaping occurred with assembly composition returning to the baseline conditions, as if neurons could opt to go in and out of the assembly depending on task conditions. A similar reshaping of neural assemblies has been postulated for motor learning in M1 of mice (Peters, Chen, & Komiyama, 2014) and remains to be explored in future analysis of our data.

Cell Activity, Hand Force and Observation

Based on the cortico-cortical and cortico-descending connections of PMd (Caminiti, et al., 2017), as well as on previous studies showing observation-related activity in this area (Cisek and Kalaska, 2004; Tkach et al., 2007), we expected that the activity of cells studied in our tasks could have been potentially related not only to hand force, but also to the observation of the cursor motion, as determined by the animal's isometric force output in different directions. Indeed, we found that, among the population of cells studied, most of them were modulated in both the hand force related tasks *(Iso, Re-Cal, Wash-out)* and in the *Obs* conditions, although with different firing rate profiles.

At population level, the strength of activation showed no significant difference between action execution, that in our study coincided with hand force change over time, and the observation of the resulting cursor's motion shown in play-back to the animals in different trials, as also observed by Cisek and Kalaska, Tkach et al. when contrasting action- and observation-related activity.

The analysis of the population of observation related-cells that were not modulated in the isometric condition (*Iso* task) showed that their activity did not change when the force field changed, therefore by task dynamics, suggesting that these cells did not encode the hand force change but merely reflected the observation in the visual space of the consequences of the force application, in terms of cursor motion in the visual field. Therefore, we can conclude that their activity encodes the observable consequence of hand-force application on the joystick, which in the real life could be represented by any object, from the robotic arms used in endoscopic surgery, to the joystick necessary to move miniature explorers or soldiers in children videogames.

In conclusion, thanks to different and apparently heterogeneous populations of cells reflecting instantaneous hand force and the resulting cursor motion, dorsal premotor cortex can encode in a coherent fashion an ethologically-relevant function consisting of hand force application on objects and monitoring its consequences in the visual world, which are important to determine objects affordance.

REFERENCES

Batschelet, E. (1981). *Circular statistics in biology* (Vol. 111, p. 388). London: Academic press.

Battaglia-Mayer, A. (2019). A Brief History of the Encoding of Hand Position by the Cerebral Cortex: Implications for Motor Control and Cognition. *Cerebral Cortex*. 29:716-731

Caminiti R, Borra E, Visco-Comandini F, Battaglia-Mayer A, Averbeck BB, Luppino G. (2017). Computational Architecture of the Parieto-Frontal Network Underlying Cognitive-Motor Control in Monkeys. *eNeuro*. 4.

Caminiti R, Ferraina S, Johnson PB. (1996). The sources of visual information to the primate frontal lobe: a novel role for the superior parietal lobule. *Cereb Cortex*. 6:319-28.

Caminiti R, Johnson PB, Galli C, Ferraina S, Burnod Y. (1991). Making arm movements within different parts of space: the premotor and motor cortical representation of a coordinate system for reaching to visual targets. *J Neurosci.* 11:1182-97.

Cheney, P. D., Fetz, E. E. (1980). Functional classes of primate corticomotoneuronal cells and their relation to active force. *Journal of neurophysiology*. 44:773-791.

Cisek P, Kalaska JF. (2004). Neural correlates of mental rehearsal in dorsal premotor cortex. *Nature*. 431:993-6.

Crammond DJ, Kalaska JF. (1996). Differential relation of discharge in primary motor cortex and premotor cortex to movements versus actively maintained postures during a reaching task. *Exp Brain Res.* 108:45-61.

Davare, M., Andres, M., Clerget, E., Tonnard, J. L. & Olivier, E. (2007). Temporal Dissociation between Hand Shaping and Grip Force Scaling in the Anterior Intraparietal Area. *J Neurosci*. 27, 3974–3980.

Dum RP, Strick PL. (1991). The origin of corticospinal projections from the premotor areas in the frontal lobe. *J Neurosci*. 11:667-89.

Dushanova, J., Donoghue, J. (2010). Neurons in primary motor cortex engaged during action observation. *Eur. J. Neurosci*. 31: 386–398.

Ehrsson HH, Fagergren E, Forssberg H. (2001). Differential fronto-parietal activation depending on force used in a precision grip task: an fMRI study. *J Neurophysiol.* 85:2613-23.

Evarts EV. (1968). Relation of pyramidal tract activity to force exerted during voluntary movement. *J Neurophysiol*. 31:14-27.

Ferrari-Toniolo S, Papazachariadis O, Visco-Comandini F, Salvati M, D'Elia A, Di Berardino F, Caminiti R, Battaglia-Mayer A. (2014). A visuomotor disorder in the absence of movement: does optic ataxia generalize to learned isometric hand action? *Neuropsychologia*. 63:59-71.

Ferrari-Toniolo, S., Visco-Comandini, F., Papazachariadis, O., Caminiti, R., & Battaglia-Mayer, A. (2015). Posterior Parietal Cortex Encoding of Dynamic Hand Force Underlying Hand–Object Interaction. *Journal of Neuroscience*, *35*(31), 10899-10910.

Ferrari-Toniolo, S., Visco-Comandini, F., Papazachariadis, O., Caminiti, R., & Battaglia-Mayer, A. (2015). Posterior Parietal Cortex Encoding of Dynamic Hand Force Underlying Hand–Object Interaction. *Journal of Neuroscience*. 35:10899-10910.

Gallese V, Fadiga L, Fogassi L, Rizzolatti G. (1996). Action recognition in the premotor cortex. *Brain*. 119:593-609.

Genovesio A, Brunamonti E, Giusti MA, Ferraina S. (2007). Postsaccadic activities in the posterior parietal cortex of primates are influenced by both eye movement vectors and eye position. *J Neurosci.* 27:3268-73.

Georgopoulos, A. P. (1992). Motor Cortex: A Changing Perspective. In R. Caminiti, P. B. Johnson, & Y. Burnod, *Control of Arm Movement in Space: Neurophysiological and Computational Approaches* (pp. 175-183). Springer-Verlag.

Georgopoulos A. P., Caminiti, R., Kalaska, J. F., (1984) Static spatial effects in motor cortex and area 5: Quantitative relations in a two-dimensional space. *Exp Brain Res* 54: 446-454.

Georgopoulos, A. P., Caminiti, R., Kalaska, J. F., & Massey, J. T. (1983). Spatial coding of movement: a hypothesis concerning the coding of movement direction by motor cortical populations. *Experimental Brain Research*, 7:327-336.

Georgopoulos AP, Kalaska JF, Caminiti R, Massey JT. (1982). On the relations between the direction of two-dimensional arm movements and cell discharge in primate motor cortex. *J Neurosci*. 2:1527-37.

Georgopoulos AP, Kettner RE, Schwartz AB. (1988). Primate motor cortex and free arm movements to visual targets in three-dimensional space. II. Coding of the direction of movement by a neuronal population. *J Neurosci*. 8:2928-37.

Georgopoulos AP, Ashe J, Smyrnis N, Taira M. (1992). The motor cortex and the coding of force. *Science*. 256:1692-5.

Hamel-Pâquet, C., Sergio, L. E., & Kalaska, J. F. (2006). Parietal area 5 activity does not reflect the differential time-course of motor output kinetics during arm-reaching and isometric-force tasks. *Journal of Neurophysiology*. 95:3353-3370.

Hatsopoulos NG, Suminski AJ. (2011). Sensing with the motor cortex. *Neuron*. 72:477-87.

Hepp-Reymond MC, Wyss UR, Anner R. (1978). Neuronal coding of static force in the primate motor cortex. *J. Physiol (Paris)*. 74:287-291.

Hepp-Reymond, M. C., Hüsler, E. J., Maier, M. A., & Qi, H. X. (1994). Force-related neuronal activity in two regions of the primate ventral premotor cortex. *Canadian journal of physiology and pharmacology*. 72:571-579.

Hepp-Reymond M, Kirkpatrick-Tanner M, Gabernet L, Qi HX, Weber B. (1999). Context-dependent force coding in motor and premotor cortical areas. *Exp Brain Res*. 128:123-33.

Innocenti GM, Caminiti R, Rouiller EM, Knott G, Dyrby TB, Descoteaux M, Thiran JP. (2018). Diversity of Cortico-descending Projections: Histological and Diffusion MRI Characterization in the Monkey. *Cereb Cortex*. 29:788-801.

Intveld RW, Dann B, Michaels JA, Scherberger H. (2018). Neural coding of intended and executed grasp force in macaque areas AIP, F5, and M1. *Sci Rep.* 8:17985.

Johnson PB, Ferraina S, Bianchi L, Caminiti R. (1996). Cortical networks for visual reaching: physiological and anatomical organization of frontal and parietal lobe arm regions. *Cereb Cortex*. 6:102-19.

Kalaska JF, R Caminiti, AP Georgopoulos (1983) Cortical mechanisms related to direction of two dimensional arm movements: Relations in parietal area 5 and comparison with motor cortex. *Exp Brain Res.* 51:247-260.

Kalaska JF, Cohen DA, Hyde ML, Prud'homme M. (1989). A comparison of movement direction-related versus load direction-related activity in primate motor cortex, using a two-dimensional reaching task. *J Neurosci*. 9:2080-102.

Kalaska, J. F., Cohen, D. A. D., Prud'Homme, M., & Hyde, M. L. (1990). Parietal area 5 neuronal activity encodes movement kinematics, not movement dynamics. *Experimental brain research*. 80:351-364.

Kalaska, J.F. and Hyde, M.L. (1985) Area 4 and area 5: differences between the load direction-dependent discharge variability of cells during active postural fixation. *Exp. Brain Res.* 59: 197–202.

Keisker, B., Hepp-Reymond, M.-C., Blickenstorfer, A. & Kollias, S. S. (2010). Differential representation of dynamic and static power grip force in the sensorimotor network. *European Journal of Neuroscience*. 31:1483–1491.

Lemon RN. (2008). Descending pathways in motor control. *Annu Rev Neurosci*. 31:195-218.

Matelli M, Luppino G, Rizzolatti G. (1985). Patterns of cytochrome oxidase activity in the frontal agranular cortex of the macaque monkey. *Behav Brain Res*. 18:125-36.

Matelli M, Luppino G, Rizzolatti G. (1991). Architecture of superior and mesial area 6 and the adjacent cingulate cortex in the macaque monkey. *J Comp Neurol*. 311:445-62.

Neely, K. A., Coombes, S. A., Planetta, P. J. & Vaillancourt, D. E. (2013). Segregated and overlapping neural circuits exist for the production of static and dynamic precision grip force. *Hum Brain Mapp.* 34: 698–712.

Peters AJ, Chen SX, Komiyama T. (2014). Emergence of reproducible spatiotemporal activity during motor learning. *Nature*. 510:263-7.

Rathelot JA, Dum RP, Strick PL. (2017). Posterior parietal cortex contains a command apparatus for hand movements. *Proc Natl Acad Sci U S A*. 114:4255-4260.

Rizzolatti G, Fadiga L, Gallese V, Fogassi L. (1996). Premotor cortex and the recognition of motor actions. *Brain Res Cogn Brain Res*. 3:131-41.

Rizzolatti G, Cattaneo L, Fabbri-Destro M, Rozzi S (2014). Cortical mechanisms underlying the organization of goal-directed actions and mirror neuron-based action understanding. *Physiol Rev.* 94:655-706.

Sergio, L. E., Hamel-Pâquet, C., & Kalaska, J. F. (2005). Motor cortex neural correlates of output kinematics and kinetics during isometric-force and arm-reaching tasks. *Journal of neurophysiology*. 94: 2353-2378.

Shmuelof L, Krakauer JW. (2011). Are we ready for a natural history of motor learning? *Neuron*. 72:469-76.

Suminski AJ, Tkach DC, Hatsopoulos NG. (2009). Exploiting multiple sensory modalities in brain-machine interfaces. *Neural Netw*. 22:1224-34.

Thach W. T., (1978). Correlation of neural discharge with pattern and force of muscular activity, joint position, and direction of intended next movement in motor cortex and cerebellum. *J. Neurophysiol.* 41:654-676.

Tkach D, Reimer J, Hatsopoulos NG. (2007). Congruent activity during action and action observation in motor cortex. *J Neurosci*. 27:13241-50.

Werner, W., Bauswein, E., Fromm, C. (1991). Static firing rates of premotor and primary motor cortical neurons associated with torque and joint position. *Experimental brain research*. 86:293-302.

Xiao J, Padoa-Schioppa C, Bizzi E. (2006). Neuronal correlates of movement dynamics in the dorsal and ventral premotor area in the monkey. *Exp Brain Res*. 168:106-19.

Ringraziamenti Accademici

Giunto al termine di questo mio percorso, desidero ringraziare anzitutto la Professoressa Alexandra Battaglia Mayer. Se è vero che la parola "tutor" racchiude molto più di una semplice trasmissione di nozioni, la Professoressa in questi tre anni me ne ha dato ampia dimostrazione. Tra tutti, non posso non riconoscerle il merito di avermi insegnato, nel senso etimologico del termine, l'importanza categorica dell'avere un metodo scientifico. Un prezioso insegnamento di cui farò tesoro, cercando di estenderlo anche al di fuori del contesto accademico poiché, come ha affermato Karl Pearson "Il metodo scientifico che esamina fatti non è tipico di una determinata classe di fenomeni e di lavoratori; è applicabile ai problemi sociali come a quelli fisici, e bisogna guardarci bene dal ritenere che uno spirito scientifico sia una peculiarità della professione di scienziato".

Un enorme ringraziamento va anche al Professor Roberto Caminiti, uomo di rara cultura e profondo conoscitore dell'*ars oratoria*. A lui, infatti, va il merito per aver svegliato e mantenuto attivo il mio interesse nei confronti della neurofisiologia, senza il quale questo lavoro non avrebbe ragion d'essere. Lavoro, tra l'altro, che ha avuto la fortuna di essere passato anche attraverso il suo attento vaglio.

Grazie alla Dottoressa Lucy Babicola, alla quale devo davvero tanto. Mi ha accompagnato all'insegna di un rapporto che oserei dire fraterno. Queste poche righe non renderanno mai giustizia a tutta la gratitudine che provo nei suoi confronti.

Un affettuoso ringraziamento è doveroso nei confronti del Dottor Luca Delle Cese, compagno di nottate di analisi e massimo complice dei risultati raggiunti. Ma più di tutti, un grande amico al quale guardo con sincera ammirazione, consapevole del fatto che una persona che fa dell'intelletto la sua arma più potente non può che vincere ogni battaglia che la vita gli pone di fronte.

Un sentito ringraziamento vuole e deve andare nei confronti di Andrea e Irene. Insostituibili compagni di viaggio che hanno allietato anche i momenti più difficili di questi tre anni. Ripenso

alle chiacchierate sui massimi sistemi, alle risate, ai momenti "ok, basta parlare di lavoro" che duravano circa 500 ms più 100 rand. Ora, quando avrò nostalgia dei nostri momenti, mi basterà ascoltare De Andrè mentre studio Arduino. Grazie, davvero.

Un ringraziamento di cuore va a Valerio e alla sua dolce metà. Il vostro affetto e il vostro supporto li sento sempre presenti, sappiatelo. Siete davvero unici e vi ringrazio per avermi motivato nei momenti più ostici.

Essendo per mia natura una persona che tende a stringere legami profondi che durano nel tempo, vorrei ringraziare il mio laboratorio d'origine. Se guardo questo lavoro, questo percorso e a cosa mi ha portato tutto questo, sento di dovervi un profondo grazie per aver fatto in modo che tutto questo iniziasse.

Ringraziamenti Personali

Il primo grazie in assoluto, com'è ovvio che sia, lo devo a mia moglie. Dicono che nella vita non ci siano certezze, che alla fin fine possa essere relegato tutto al beneficio del dubbio. Io una certezza ce l'ho. Una sola. E questa sei tu. Grazie per tutto quello che hai fatto, per quello che fai e che sei ogni giorno. Grazie per il supporto, per quando raccogli i miei cocci e con pazienza li rimetti insieme. Grazie per le risate, ormai componente indispensabile delle nostre giornate. Grazie per il tuo amore, che è il motore primo della mia vita.

Un grazie infinitamente grande ad una personcina ancora infinitamente piccola. Spero che un domani, leggendo queste righe, ti possa rendere conto di quanto mamma e papà si vogliano bene, e di quanto ti vogliano bene già da adesso. Grazie per averci cambiato la vita, Arianna.

Grazie a mamma e a papà. Ancora una volta, ancora un grazie, ma non saranno mai abbastanza per quanto mi riguarda. Guardando questo risultato, non siate fieri di me, ma di voi, perché abbiate l'intima consapevolezza che come genitori siete insuperabili. Vi voglio bene, e anche questo non mi stancherò mai di ripeterlo. Grazie.

A Serena, Simone, Giandomenico, Desirèe, Camilla e Luca un ringraziamento per regalare sale alla mia esistenza. La mia famiglia, il mio porto sicuro, eppure anche i miei amici e i miei complici. Come è possibile mi chiederete? Non ne ho idea, so solo che funziona così, e non lo cambierei per nulla al mondo.

Un grazie a tutto il resto della mia mega-famiglia, che mi segue in tutte le tappe importanti continuando a regalarmi positività.

Grazie a tutti i miei amici. Le persone crescono, la vita cambia, ma alcune cose restano vere per quello che sono. È il caso delle amicizie profonde, che restano uguali a sé stesse pur crescendo con te, dimostrando che è proprio questa la loro forza. Ti danno la consapevolezza del fatto che se ti ritrovi a dover tagliare il più possibile i ringraziamenti perché vorresti dire grazie ad ogni singola persona, è perché hai sempre ricevuto affetto da tutti, e vorresti solo ricambiarlo. A voi tutti, Grazie.